JOURNAL OF MATERIALS SCIENCE 28 (1993) 2035–2039

Solid state electrochemical CO_2 gas sensor using zircon-based sodium ionic conductors

Y. SADAOKA*, M. MATSUGUCHI, Y. SAKAI, D. MANABE
Department of Applied Chemistry, Faculty of Engineering, Ehime University, Matsuyama, 790 Japan

The sensing properties and characteristics of a zircon-based sodium ionic conductor as an electrochemical CO_2 gas sensor which can be expressed as

$$O_2, \mathrm{Pt}|\mathrm{Na\ ion\ conductor}|\mathrm{Pt}, Na_2CO_3, CO_2, O_2$$

were examined. The electro motive force (e.m.f.) was found to be a function of the logarithm of CO_2 concentration and the 90% response time was less than 2 min at 430 °C while the number of electrons for the electrochemical reaction was slightly above than 2. The coexistence of water molecules ($\geqslant$ 90% RH) induced the response time delay and the lowering of the e.m.f. value. Changes in the response characteristics were mostly recovered after cutting off the water vapour, while the recovery time was prolonged when the working temperature was increased.

1. Introduction

The discovery of $Na_3Zr_2Si_2PO_{12}$ represented an important development in the field of solid electrolytes because it demonstrated that a three-dimensional framework structure was comparable to that of β-alumina. It has been shown that crystalline compounds with the composition $Na_{1+x}Zr_2Si_xP_{3-x}O_{12}$ belong to the best fast sodium-ion conductors. The compositions with the highest ionic conductivities are the original solid solution system with $1.8 \leqslant x \leqslant 2.4$ [1, 2]. Recently, there has been considerable interest in dense superionic conductors for solid state batteries and/or electrochemical gas sensors for NO_x. SO_x, CO_2 [3–6], while the chemical stability of $Na_3Zr_2Si_2PO_{12}$ is superior but it is very difficult to prepare as dense plates. It has been reported previously [7] that the sintered zircon–sodium phosphate mixture is a high sodium ionic conductor and the addition of sodium phosphate is effective in fabricating a dense fast sodium ionic conductor and in decreasing the sintering temperature necessary to obtain the reactants. Similar fabrication of an ionic conductor was reported by Saito *et al.* [8], and its subsequent application to an electrochemical SO_x sensor.

The present paper presents results of a study of the zircon-based sodium ionic conductor for a solid state electrochemical CO_2 gas sensor in which Na_2CO_3 was coated on the working electrode.

2. Experimental procedure

Fine-particle zircon (mean particle size 1–2 μm), dibasic sodium phosphate and phosphoric acid were used. The raw materials were weighed in the prescribed mole ratio and mixed with water as a mixing medium. Preparation conditions with respect to composition are summarized in Table I. After evaporation of the water, the mixed powder was pressed into disc form, and dried at 400 °C for 2 h. After grinding in by a vibrating mill, the powder was pressed into a disc and was finally sintered at 1000 °C in air for 24 h. Platinum paste was painted to opposite faces of the disc (10 mm diameter and 0.4 mm thick) and platinum wires were set in place. After drying, the sample was heated at 800 °C for 30 min to fix the electrodes and wires. The element was attached to the top of an alumina tube (10 mm diameter) using an inorganic adhesive (Sauereisen) and dried at 80 °C for 8 h. A sodium carbonate layer was prepared on the outside electrode by droping Na_2CO_3 solution followed by drying. Standard gases of synthesized air with 10, 100, 1000 p.p.m. or 1% CO_2 were introduced to the

TABLE I Components of starting materials and electrical characteristics of electrolyte observed above T_v

Specimen	Raw materials(mole)			Conductivity at 300 °C ($S\ cm^{-1}$)	Activation energy(eV)	T_v (K)
	$ZrSiO_4$	Na_2HPO_4	H_3PO_4			
ZPNa10	1	0.150	0.420	2.6×10^{-3}	0.30	493
ZPNa20	1	0.300	0.370	1.4×10^{-2}	0.22	463
ZPNa33	1	0.495	0.305	4.7×10^{-3}	0.32	493
ZPNa50	1	0.750	0.220	1.6×10^{-4}	0.43	493

0022–2461

working electrode side (outside) and synthesized air or compressed air to the reference electrode side (inside). The impurity concentration of synthesized air was as follows: CO < 1 p.p.m., CO_2 < 2 p.p.m., HCl < 1 p.p.m. and H_2O < 10 p.p.m. The humidity of the objective gases was controlled by allowing gases to bubble or pass through liquid water and it was then calibrated using a capacitive-type humidity sensor and by measuring the dew point. The electromotive force of the sensor was measured using a digital electrometer. All the measurements were controlled using a personal computer. The electrical characteristics were examined by complex impedance analysis. The crystalline phases were identified at room temperature by the standard X-ray diffraction technique. The microstructures were examined by scanning electron microscopy (SEM).

3. Results and discussion

3.1. Electrical properties

Complex-plane impedance plots were applied to determine the conductivity. In the lower temperature region for ZPNa50, the high-frequency results were represented by arcs and the low-frequency ones by spurs. With an increase in the measuring temperature, the arcs were diminished and only quasi-straight lines were observed. For the sample with a lower sodium phosphate content, such as ZPNa-10, 20 and 33, only quasi-straight lines were observed at 80 °C or more. From these results the resistance component was derived from an extrapolation to zero reactance of the impedance plot. The conductivity data were related by the Arrhenius equation

$$\sigma T = \sigma_0 \exp(-E/kT) \qquad (1)$$

where σ is the conductivity, σ_0 is the pre-exponential factor, E is the activation energy, k is the Boltzmann constant and T is the absolute temperature. The activation energy for the ionic conduction changes in the temperature range 450–500 K(T_v) and the activation energy in the higher temperature region is lower than that in the lower region. The electrical characteristics are summarized in Table I. Except for ZPNa50, the estimated activation energies for conductivity were comparable to the literature values of about 0.36 eV in a lower temperature region and 0.21 eV in a higher temperature region for $Na_3Zr_2Si_2PO_{12}$ [9]. While the pre-exponential factor increased with sodium content, the highest conductivity and the lowest activation energy were achieved for ZPNa20.

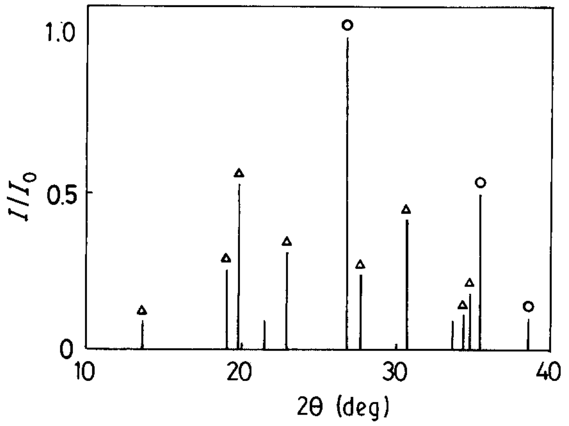

Figure 1 XRD pattern of ZPNa20. (○) $ZrSiO_4$, (△) $Na_3Zr_2Si_2PO_{12}$.

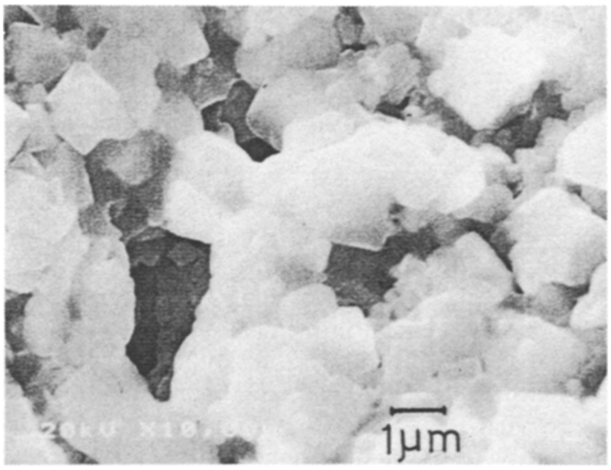

Figure 2 Microphotograph of ZPNa20.

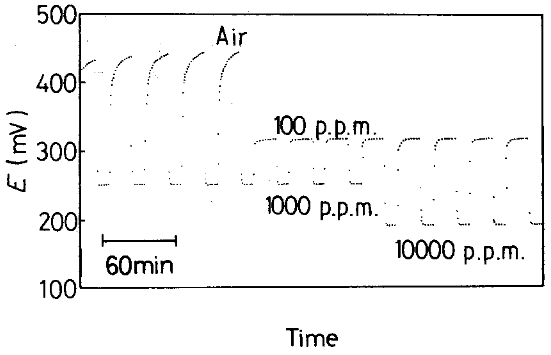

Figure 3 Repeated response curve of the e.m.f. for CO_2 changes at 417 °C. Synthesized air was passed to the reference electrode side. The concentration of CO_2 was as denoted in the figure.

3.2. XRD and SEM results

From the X-ray diffraction pattern of ZPNa20, it was confirmed that the reactant after sintering was a mixture of $Na_3Zr_2Si_2PO_{12}$ and $ZrSiO_4$ as shown in Fig. 1. The peak height at $2\theta = 26.8°$ assigned to $ZrSiO_4$ was twice as high as that at $2\theta = 19.8°$ assigned to $Na_3Zr_2Si_2PO_{12}$. The microstructure of ZPNa20 was observed by SEM and the result is shown in Fig. 2. The sintering proceeded, but some micropores were not removed. The size of the ZPNa20 particles was similar to that of the zircon powders as starting materials. It appears that $Na_3Zr_2Si_2PO_{12}$ layers are formed on the surface of the zircon particles.

3.3. CO_2 sensing characteristics

Fig. 3 shows the sensing characteristics at 417 °C for the sensor fabricated with ZPNa20. In this case, synthesized air (50 ml min^{-1}) was passed through

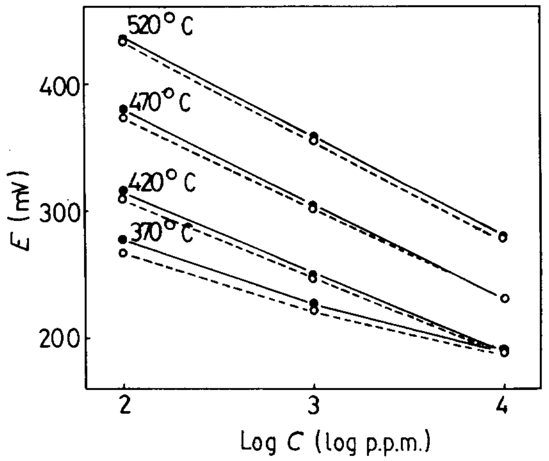

Figure 4 CO_2 concentration dependence of the e.m.f. at certain temperatures, in (—) synthesized air or (. . . .) 380 p.p.m. CO_2/air which were passed to the reference electrode side. Temperature was as denoted in the figure.

the reference electrode side. On switching from 1000 p.p.m. CO_2/air flow to air flow, the e.m.f. increased quickly while a steady state value was not observed in the measuring period (20 min). Except for the case of switching from air containing CO_2 gas to synthesized air, the response and recovery times were very fast; the 90% response time was less than 2 min. The response and recovery characteristics observed when air with 380 p.p.m. CO_2 was passed through the reference electrode side were in fair agreement with the results when synthesized air was passed through, while the e.m.f. values in the former case were slightly lower than those in the latter case, as shown in Fig. 4. The difference between the e.m.f. values observed in both cases decreased with increase in the operating temperature and CO_2 concentration of the objective gas. The sensitivity (ΔE, mV/decade), i.e. the slope shown in Fig. 4, and the e.m.f. value increased with increasing working temperature, while the observed sensitivity was slightly smaller than the theoretical value for the two-electron electrochemical reaction. In addition, the degree of deviation between the observed and theoretical values increased with decreasing working temperature. The electron number for the reaction was ~ 2.1 at 520 °C; this monotonically increased to 2.7 at 370 °C with decreasing temperature. Furthermore, the response time shows a tendency to become faster with increasing operating temperature.

The presence of water vapour influenced to the sensing characteristics. The sensing characteristics were mostly uninfluenced by the existence of water vapour (15 °C dew point) at 436 °C, as shown in Fig. 5a and b. However, when the working temperature increased and the water concentration increased to a dew point of 27 °C or more, the response time became slower and the e.m.f. decreased, as shown in Fig. 6a and b. Fig. 6 shows the sensing characteristics observed at 495 °C. The introduction of water vapour induced the lowering of the e.m.f., while a rapid recovery was confirmed when the water vapour was removed. When the working temperature was raised to 520 °C, a larger decrement in the e.m.f. value was observed by the introduction of water vapour, but this drift was not caused by the permanent deformation of the sensor because the sensing characteristics were recovered after cutting off the water vapour while the recovery time became longer.

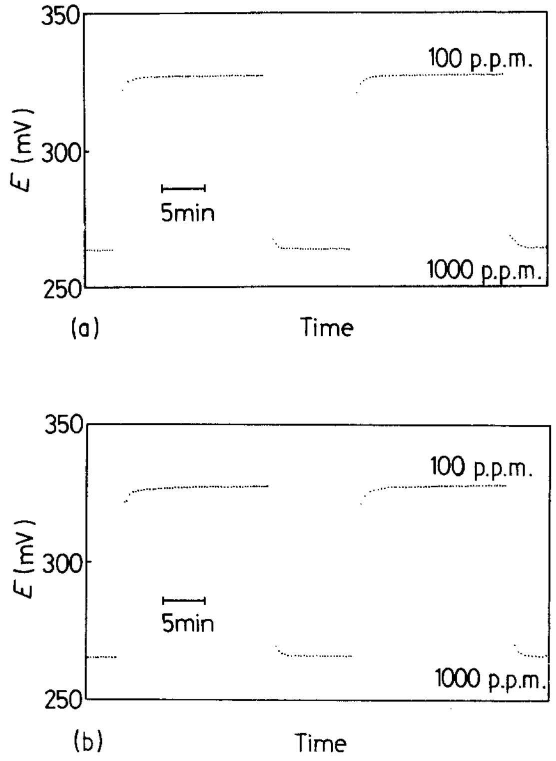

Figure 5 Response curve of the e.m.f. for CO_2 changes from 1000 p.p.m. to 100 p.p.m. and inversed at 436 °C. (a) Dried CO_2/air, (b) CO_2/air with 15 °C dew point.

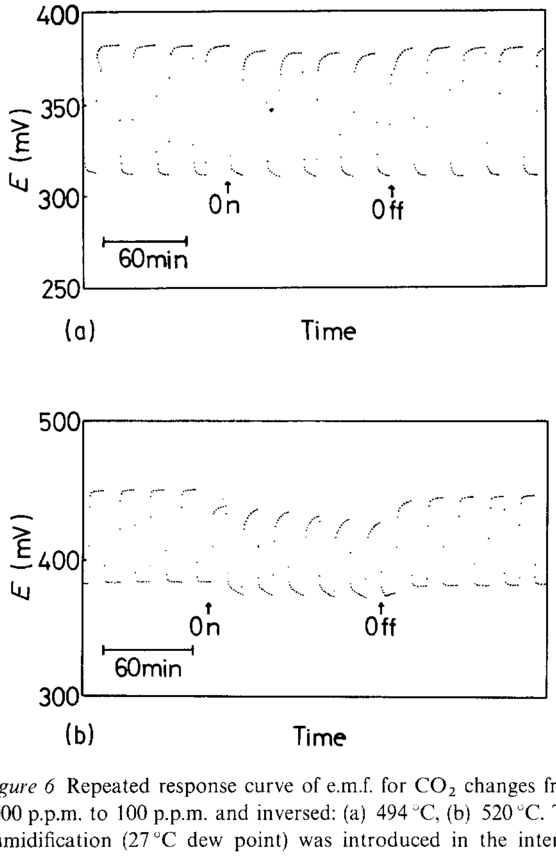

Figure 6 Repeated response curve of e.m.f. for CO_2 changes from 1000 p.p.m. to 100 p.p.m. and inversed: (a) 494 °C, (b) 520 °C. The humidification (27 °C dew point) was introduced in the interval between on and off.

The fabricated electrochemical CO_2 sensor may be expressed as

$$O_2, Pt|Na \text{ ion conductor}|Pt, Na_2CO_3, CO_2, O_2$$

In this case, the left-hand side acts as a reference electrode and the right-hand side as a working electrode. As is well-known [10], a two-electron reaction in the working electrode is conventionally written as

$$2Na^+ + CO_2 + (1/2)O_2 + 2e^- = Na_2CO_3 \qquad (2)$$

whereas the reference electrode reaction is expressed by the equation

$$2Na^+ + (1/2)O_2 + 2e^- = Na_2O \text{ (in electrolyte)} \qquad (3)$$

The overall reaction is reduced to

$$Na_2CO_3 = Na_2O + CO_2 \qquad (4)$$

When the activity of Na_2CO_3 is kept constant, as is the partial pressure of oxygen on both atmosphere sides, the e.m.f. can be expressed as

$$E = E_0 - (RT/2F)\ln(a_{Na_2O}P_{CO_2}) \qquad (5)$$

where P_{CO_2} is the partial pressure of CO_2, E_0 a constant, a_{Na_2O} the activity of Na_2O, and RT/F has the usual meaning. The thermodynamically most stable compound is Na_2CO_3 in this system, but Na_2O, Na_2O_2 are also possibly formed because of higher kinetic preferences. Furthermore, the formation of NaOH and $NaHCO_3$ is also possible, especially in the presence of water vapour.

If Na_2O, Na_2O_2 and Na_2CO_3 are formed simultaneously by the cell reactions in the presence of CO_2

$$4Na^+ + CO_2 + (3/2)O_2 + 4e^- = Na_2CO_3 + Na_2O_2 \qquad (6)$$

$$3Na^+ + CO_2 + O_2 + 3e^- = Na_2CO_3 + (1/2)Na_2O_2 \qquad (7)$$

the sensitivity may be lower than the theoretical value for the two-electron process [2] and the galvanic cell will show characteristics of mixed potentials which are given by the relative contributions of the Gibbs energies of formation of the sodium carbonate and the oxides. Recently, Liu and Weppner [10] have reported that the sensitivity for CO_2 of the galvanic cell with β″-alumina coated with Na_2CO_3 at 150 °C, is less than the theoretical value for the two-electron process and the formation of sodium oxides is considered to be the origin of the difference. In fact, the Gibbs energy and the enthalpy at 298 K are -375 and $-414\,kJ\,mol^{-1}$ for Na_2O, -448 and $-511\,kJ\,mol^{-1}$ for Na_2O_2 and -1044 and $-1130\,kJ\,mol^{-1}$ for Na_2CO_3. The enthalpy for the reactions is

$$Na_2O + CO_2 = Na_2CO_3 \qquad \Delta H = -323\,kJ\,mol^{-1} \qquad (8)$$

$$Na_2O_2 + CO_2 = Na_2CO_3 + (1/2)O_2 \qquad \Delta H = -227\,kJ\,mol^{-1} \qquad (9)$$

The enthalpy value for Equation 9 is considerably smaller than that for Equation 8. The formation of Na_2O_2 can be depressed by increasing the working temperature.

The formation of $NaHCO_3$ and NaOH may proceed in the presence of water vapour. The enthalpy for the reactions is

$$Na_2O + H_2O = 2NaOH \qquad \Delta H = -194\,kJ\,mol^{-1} \qquad (10)$$

$$Na_2O_2 + CO_2 + H_2O = NaHCO_3 + NaOH \qquad \Delta H = -230\,kJ\,mol^{-1} \qquad (11)$$

$$NaOH + (1/2)CO_2 = (1/2)Na_2CO_3 + (1/2)H_2O \qquad \Delta H = -64\,kJ\,mol^{-1} \qquad (12)$$

$$NaOH + CO_2 = NaHCO_3 \qquad \Delta H = -132\,kJ\,mol^{-1} \qquad (13)$$

$$NaHCO_3 + (1/2)Na_2O = Na_2CO_3 + (1/2)H_2O \qquad \Delta H = -94\,kJ\,mol^{-1} \qquad (14)$$

$$NaHCO_3 + (1/2)Na_2O_2 = Na_2CO_3 + (1/2)H_2O + (1/4)O_2 \qquad \Delta H = -45\,kJ\,mol^{-1} \qquad (15)$$

All the above reactions take negative values of enthalpy, while the reaction

$$2NaHCO_3 = Na_2CO_3 + H_2O + CO_2 \qquad \Delta H = +136\,kJ\,mol^{-1} \qquad (16)$$

takes a positive value. From thermodynamic considerations, NaOH and $NaHCO_3$ may be removed as the result of the reaction with CO_2 and sodium oxides. Whilst it is expected thermodynamically that the formation of Na_2CO_3 from $NaHCO_3$ is impossible because the enthalpy is positive, the self decomposition of $NaHCO_3$ occurs at 270 °C or more. When the working temperature is higher than 270 °C or more, the drift of the e.m.f. caused by the coexistence of water vapour can be recovered after cutting off the water vapour in the objective gases. Recovery of the sensitivity after water vapour cut-off was very fast for the sensor operated at 500 °C or lower, but was not so fast at 520 °C or more as shown in Fig. 6. With increasing working temperature, the water molecules and CO_2 are able to diffuse more easily into the solid electrolyte and this results in the formation of Na_2CO_3 and NaOH species on the grain boundary (NASICON layer). The diffusion of CO_2 may be accelerated by the existence of water, because the CO_3^- ion is formed. In extreme cases, the activity of the sodium ion may be varied by the formation of other new compounds such as Na_2CO_3 and NaOH in the electrolyte (consumption of sodium oxides in the electrolyte) which results in permanent drifts of the sensing characteristics.

Furthermore, it is noted that the critical temperature of phase transition of Na_2CO_3 is 450 °C, while the enthalpy of phase transition is not so high ($0.690\,kJ\,mol^{-1}$). The reproducibility and stability for thermal cycling may be influenced by the phase transition of $NaCO_3$ when the sensor is operated at

450 °C or more. In fact, thermal cycling from room temperature to 470 °C induced a lack of the reproducibility of the sensing characteristics caused by peeling of the Na_2CO_3 and, in extreme case, platinum layers also.

4. Conclusions

We have examined an electrochemical CO_2 gas sensor using a zircon-based sodium ionic conductor. The characteristics of this sensor were as follows.

1. The prepared ionic conductor was a mixture of zircon and $Na_3Zr_2Si_2PO_{12}$ and the electrical characteristics of ZPNa20 were $0.01\ S\ cm^{-1}$ at 300 °C for conductivity and 0.22 eV for activation energy, which are comparable to dense $Na_3Zr_2Si_2PO_{12}$ singly.

2. The electrochemical sensor prepared with the working electrode coated with Na_2CO_3 shows a Nernst response to CO_2 and the electron number is estimated to ~ 2.1 at 470 °C; the number increases with decreasing working temperature. At lower temperature, the formation of sodium oxides at the working electrode may occur.

3. The existence of water vapour in the objective gases induce a slight decrease in e.m.f., while this change is recovered after water vapour cut-off. The recovery time is very fast at 500 °C or below, and becomes longer with increasing working temperature which may be correlated with the diffusion of water molecules and $CO_3^{=}$ into the bulk along the grain boundary.

References

1. J. B. GOODENOUGH, H. Y. P. HONG and J. A. KAFALS, *Mater. Res. Bull.* **11** (1976) 203.
2. U. von ALPEN, M. F. BELL, R. BRÜTIGAN and H. LAIG-HÖRSTEBROCK, in "Fast Ion Transport in Solids", edited by V. Vashista, J. N. Mundy and G. K. Shenoy (North Holland, Amsterdam, 1979) p. 443.
3. M. GAUTHIER and A. CHAMBERLAND, *J. Electrochem. Soc.* **124** (1977) 1579.
4. G. HÖTZEL and W. WEPPNER, *Solid State Ionics* **18**, **19** (1986) 1223.
5. R. AKILA and K. Y. JACOB, *J. Appl. Electrochem.* **18** (1988) 245.
6. S. YAO, Y. SHIMIZU, N. MIURA and N. YAMAZOE, *Chem. Lett.* (1990) 2033.
7. Y. SADAOKA and Y. SAKAI, *J. Mater. Sci.* **20** (1985) 3027.
8. Y. SAITO, T. MARUYAMA, Y. MATSUMOTO and Y. YANO, in "Proceedings of the International Meeting on Chemical Sensors" (Kodansha, Elsevier, Tokyo, 1983) p. 326.
9. U. von ALPEN, M. F. BELL and W. WICHELHANS, *Mater. Res. Bull.* **14** (1979) 1317.
10. J. LIU and W. WEPPNER, *Solid State Commun.* **76** (1990) 311.

Received 6 August 1991
and accepted 24 March 1992